Laser and Particle Beams (2003), *21*, 633–638. Printed in the USA.

DOI: 10.1017/S0263034603214233

High-current laser ion source based on a low-power laser

M. OGAWA,[1] M. YOSHIDA,[1] M. NAKAJIMA,[2] J. HASEGAWA,[1] S. FUKATA,[1]
K. HORIOKA,[2] AND Y. OGURI[1]

[1]Research Laboratory for Nuclear Reactors, Tokyo Institute of Technology, Meguro, Tokyo 152-8550 Japan
[2]Department of Energy Sciences, Tokyo Institute of Technology, Nagatsuta, Yokohama, 226-8501 Japan

(RECEIVED 27 May 2003; ACCEPTED 11 November 2003)

Abstract

An ion source for generation of low-charged heavy ions has been developed using low-power KrF excimer and frequency-doubled Nd:YAG lasers. The ion source was examined with two experimental modes of low-voltage DC extraction at ~20 kV and high-voltage pulse extraction at 150 kV. Normalized emittance of extracted beams composed of Cu^+ and Cu^{2+} ions was measured to be about 0.05 and 0.8 πmm-mrad for the DC extraction and the pulse extraction, respectively. Electron temperature was observed by means of a single probe method to be 0.8 to 2.5 eV, depending on the intensity of the KrF laser.

Keywords: emittance; heavy ion; KrF; laser; Nd:YAG; plasma; source; temperature

1. INTRODUCTION

A heavy ion fusion (HIF) scenario is based on techniques of very intense heavy ion beams, which can deliver energy of several megajoules to fusion target during a time of about 10 ns. There are many technical issues about the beams that must be solved to realize the HIF driver. The high-current beams relevant to the HIF suffer from a very strong space charge effect, leading to serious deterioration of beam quality not only at beam acceleration but also at beam transport. The space charge effect is strong in particular when the ion velocities are low. To overcome the space charge effect, the current design of energy drivers based on induction accelerators adopts multistage linear accelerators where several beams from a low-energy section are merged and then injected to the succeeding stage (Bangerter, 1999). A large number of ion sources share the required beam intensities at the lowest energy section.

The scheme of the multistage design requires ion sources that can generate about 10^{14} heavy ions over a time duration of several microseconds. The macro energy carried by the beam pulse is defined by the number of ion particles in the pulse. So it is essential for the HIF to supply the ion beams of high particle density. Laser ion sources have the potential for providing the intense heavy ion beams. The conventional laser ion sources have so far been aimed at generation of high-charged ions by irradiating infrared laser light from a high-power CO_2 laser (Sharkov *et al.*, 1998).

On the other hand, the inverse bremsstrahlung process forming ablation plasmas by laser irradiation gives the following equation for plasma temperature of T_e; $T_e \propto (I\lambda^2)^{2/3}$ where I is laser intensity and λ wavelength of laser light (Henkelmann *et al.*, 1992; Mora, 1982). This equation allows us to generate the ablation plasmas with low temperature by using a low-power laser of short wavelength. In fact, several groups have observed low-charged ions such as Cu^+, Fe^+, Fe^{2+}, Al^+, and Al^{2+} by using low-power UV and visible lasers (Amoruso *et al.*, 1996; Tyrrell *et al.*, 1996). However, the electron temperature of the ablation plasma was not measured in connection with the ion production. The low-temperature plasma provides the heavy ions of low-charge states such as 1+ and 2+. So we have begun to develop a laser ion source generating high-current beam of low-charged heavy ions (Hasegawa *et al.*, 2000; Yoshida *et al.*, 2000, 2001). The beam of low-charged ions has an advantage to minimize the space charge effect for a fixed particle density of the beam. Moreover the plasma of low temperature leads to low emittance of the beam.

However, it is important to balance the plasma density and the ion extraction to achieve good optical conditions. The optically good beam is obtained by matching of beam perveance, that is, by optimizing the extraction voltage to the ion supply from the plasma. We examine the role of drift space, which adjusts the ion density in the expanding plasma

Address correspondence and reprint requests to: Masao Ogawa, Research Laboratory for Nuclear Reactors, Tokyo Institute of Technology, 2-12-1 Oohkayama, Meguro-ku, Tokyo 152-8550 Japan. E-mail: mogawa@nr.titech.ac.jp

to the ion extraction. The beam quality is also affected by the characteristics of the laser plasma. So it is worth studying the behavior of ions emerging from the laser plasma by measuring the electron temperature of the ablation plasma and the emittance of the extracted beams (Roudskoy, 1992).

2. EXPERIMENTS AND RESULTS

Ablation plasmas containing low-charged copper ions were generated using low-power lasers. Our laser ion source was tested for two extraction modes, that is, low-voltage DC extraction and high-voltage pulse extraction.

2.1. Low-voltage extraction

For experiments of DC voltage extraction, we used a KrF excimer laser that can provide laser pulses of $\lambda = 248$ nm with energy in the range of 150 mJ to 350 mJ per pulse. FWHM width of the laser pulse was 30 ns. Figure 1 shows a schematic view of the ion source. A copper disc placed in vacuum was irradiated with the laser at an incident angle of 60°. A typical spot size of the laser light on the copper target was in the elliptical shape of $0.34 \times 0.025\ \pi\text{cm}^2$. About 30% of the initial laser energy was absorbed through the air and the quartz window. The irradiation density of the laser on the target was varied from 1.4×10^8 to 3.2×10^8 W/cm^2. The ablation plasmas were freely expanded in a drift chamber to dilute the ion density because the plasma density in the vicinity of the copper target was too high to extract the ions at the low voltage. Before determining the drift distance, we measured the ion flux in the plasma as a function of the distance from the target. The drift distance of 65 cm was chosen so that the ion current density at the extraction gap of 18 mm did not exceed the space-charge limited current density. Both anode and cathode electrodes had apertures of 10 mm in diameter. The extracted ion current was observed with a Faraday cup placed at 10 mm behind the cathode electrode. The extraction voltage was so optimized to obtain the current profiles having approximately the flat-top region after the initial peak for several microseconds. We scanned the laser irradiation density at four values. The four cases of the perveance matching that we adopted in this work are given in Table 1. As the laser intensity increased, the plasma density became higher. Then the higher extraction voltage was necessary to balance the ion supply with the ion extraction. Figure 2 shows the typical profiles of the extracted ion current density. It is noted that the current density of $\sim$70 mA/cm^2 was achieved at the irradiation power density of 3.2×10^8 W/cm^2.

The electron temperature of the ablation plasma was diagnosed with the Langmuir single probe method because its applicability to the plasma plumes with the significant drift velocities had been demonstrated by von Gutfeld and Drefus (1989) and by Weaver *et al.* (1999). Because the electron temperature of about 1 eV was estimated for the plasma plume formed with a UV laser of $\lambda = 351$ nm (Amoruso *et al.*, 1996), we expected to apply this method to the present ablation plasma. A single probe of 0.2 mm in diameter and 5 mm in length was placed 30 mm downstream from the copper target. The electron temperature was measured as a function of time for the different laser conditions. The highest values of the temperatures were observed at about 1 μs after the laser irradiation when the ablation front traveled the drift distance with a drift velocity of $\sim 3 \times 10^4$ m/s. For the cases of 1.4×10^8 and 3.2×10^8 W/cm, the electron temperatures sank to a level of 0.5 eV at 2 μs and then decreased gradually with time. The temperature went down after the ablation front passed the probe. The electron temperatures obtained at 1 μs after the laser irradiation are plotted in Figure 3 as a function of the laser intensity. A dotted line in the figure indicates the above equation of $\propto I^{2/3}$, which roughly reproduces the experimental results.

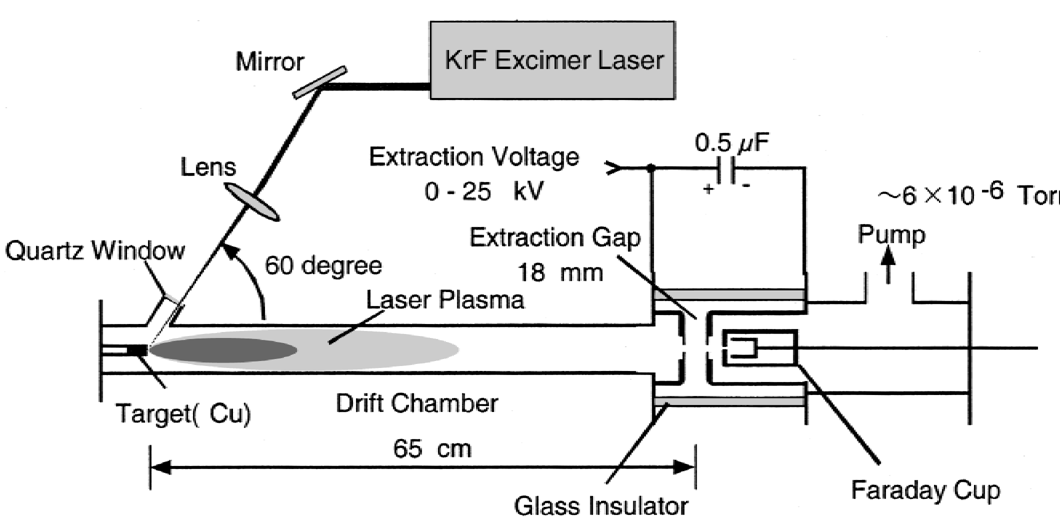

Fig. 1. A schematic view of laser ion source at low-voltage DC extraction.

https://doi.org/10.1017/S0263034603214233 Published online by Cambridge University Press

Table 1. *Four combinations of laser irradiation density and extraction voltage for optimized beam extraction*

Case	Laser power density (10^8 W/cm^2)	Extraction voltage (kV)
a	1.4	13
b	2.2	19
c	2.5	21
d	3.2	24

Emittance of the extracted beams was measured with the pepper-pot method. A disc having 89 holes of 200 mm in diameter with spacing of 2 mm was set 10 mm behind the cathode. The ions having passed through the pepper-pot disc were detected with a microchannel plate backed by a phosphor screen. The detector was biased with a high-voltage pulse of 100 ns duration to record the time-resolved ion images. The images of the beamlets were taken with a streak camera. The beamlet images were converted to the emittance in terms of the equation proposed by Wang *et al.* (1991). The normalized emittance values are illustrated in Figure 4 for three laser irradiation conditions. It is noted that the observed emittance values are as low as 0.05 πmm-mrad at about 30 μs when the beam current profiles in Figure 2 show approximately the flat-top.

2.2. High-voltage extraction

The ion source was also examined with the pulse extraction at a voltage of 150 kV. An experimental setup is depicted in

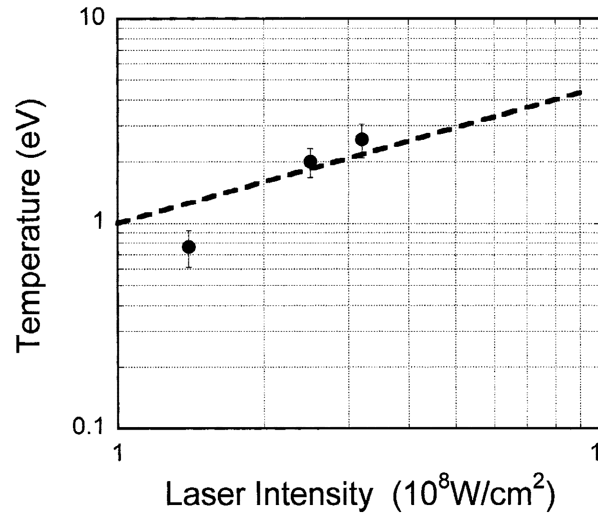

Fig. 3. Electron temperature of ablation plasma measured as a function of irradiation power density of a KrF laser. A dotted line indicates fitting to $T_e \propto I^{2/3}$.

Figure 5. The high-voltage pulse was generated with an induction adder consisting of four induction modules. The pulse width was 400 ns. The laser target of copper plate was mounted on the end of the high-voltage rod, which functioned as the anode. The cathode electrode having an aperture of 10 mm in diameter was placed at 20 mm from the anode. The copper plate was irradiated with a frequency-doubled Nd:YAG laser of $\lambda = 532$ nm with pulse width of 6 ns. The laser spot had the elliptical shape of 0.16 $\times$ 0.07 πcm^2. The acceleration gap of 10 mm spacing was located 12 mm downstream from the copper target. In the case of the pulse mode, the quality of the extracted beam was strongly

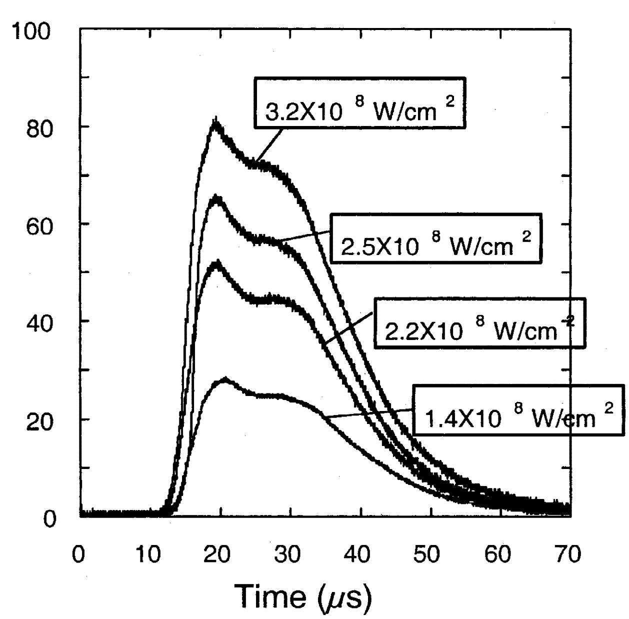

Fig. 2. Time evolution of current densities of copper beams extracted from ablation plasmas formed by a KrF laser with different irradiation power densities.

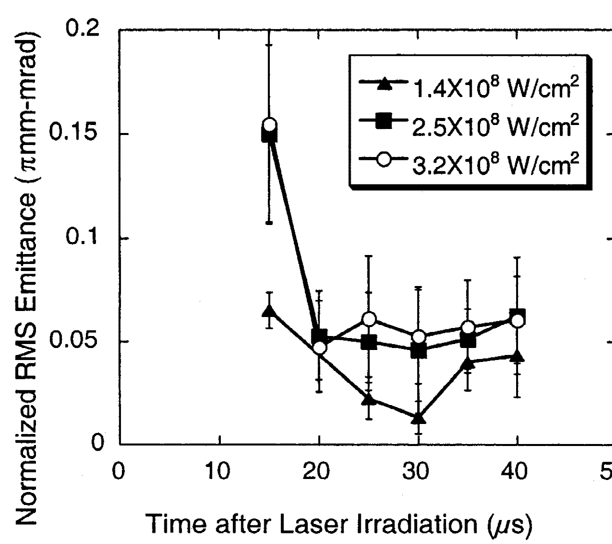

Fig. 4. Time evolution of normalized root-mean-square emittance measured for three different combinations of laser power density and extraction voltage.

https://doi.org/10.1017/S0263034603214233 Published online by Cambridge University Press

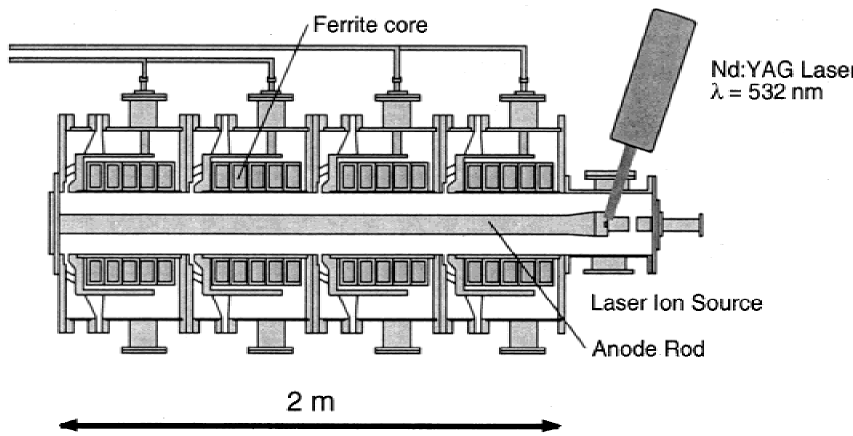

Fig. 5. A schematic view of laser ion source mounted on a high-voltage induction adder.

dependent on the timing of the ion extraction. The extracted beam current was measured with a Faraday cup directly connected to the cathode. The Faraday cup had an entrance aperture of 10 mm in diameter. For formation of the cold plasmas, we examined the ion source at the low irradiation power in the vicinity of the threshold to generation of the ablation plasma. Figure 6 indicates the plasma ion current and the extracted beam current measured as a function of laser energy near the threshold of the ablation plasma formation. The plasma ion current increased nonlinearly from 0 to 1 A with the laser energy. On the other hand the extracted beam current reached a plateau at a laser energy of 40 mJ, that is, the irradiation density of 1.9×10^8 W/cm^2. Figure 7 shows the time evolution of the extracted beam currents observed at three typical timings of the extraction voltage where the laser intensity was fixed to 53 mJ, that is, 2.5×10^8 W/cm^2. When the timing of the extraction voltage was delayed to the plasma ion current profile, the extracted beam current showed a spike followed by its tail. The preceding timing did not provide the rectangular profile of the extracted beam current. Only when the extraction voltage was coincident with the peak in the plasma ion current profile, the rectangular shape of the ion extraction was achieved. It is noteworthy that the fastest rise time of the extracted beam profile obtained was about 30 ns at a laser energy of 53 mJ. At the optimal timing, the beam divergence was smallest.

The emittance of the accelerated beam was measured in the same way as the case of the low-voltage extraction using the pepper-pot method. The pepper-pot disc was placed 5 mm from the cathode. The microchannel plate detector was set 15 mm downstream from the cathode. Figure 7 shows the normalized emittance obtained as a function of the laser energy. The emittance was dependent on the laser energy. The lowest emittance was 0.8 πmm-mrad with a laser energy of 53 mJ, which produced the plasma ion current density of 0.7 A/cm^2 (Fig. 6).

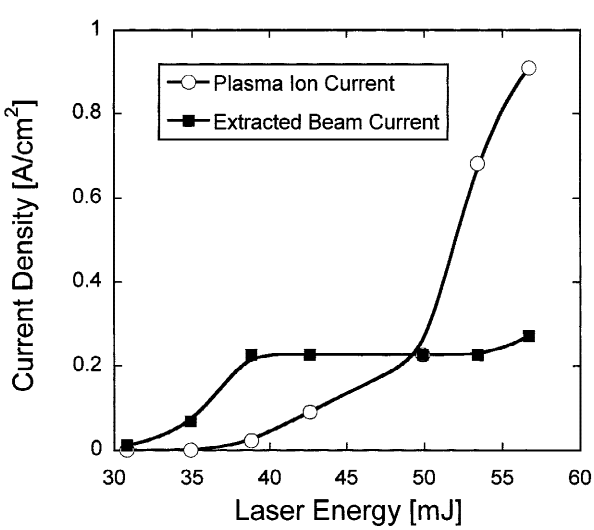

Fig. 6. Plasma ion current and extracted beam current measured as a function of Nd:YAG laser energy per pulse near the threshold of ablation plasma formation.

3. DISCUSSION

We have produced predominantly ions of Cu^+ and Cu^{2+} with the laser ion sources driven by the low-power KrF excimer and frequency-doubled Nd:YAG lasers. This observation is in agreement with other studies. Tyrrell *et al.* (1996) measured energies of Cu^+ ions from ablation plasma formed by a KrF excimer laser with an irradiation density of 0.5×10^8 to 3.5×10^8 W/cm^2. Amoruso *et al.* (1996) observed a high production ration of Al^+ to Al^{2+} at a power density of $\sim 1 \times 10^8$ W/cm^2 with a XeF laser of $\lambda = 351$ nm. A calculation based on the database (Group T4, 2002) shows that a plasma with a density of 10^{18} cm^{-3} leads to a mean ion charge of 1.5, that is, Cu^+:$Cu^{2+} \approx 1$:1, at a temperature of 2 eV.

The electron temperatures measured for the ablation plasma are explained in terms of the equation of $T_e \propto I^{2/3}$ as shown in Figure 3. This supports the picture of the inverse

https://doi.org/10.1017/S0263034603214233 Published online by Cambridge University Press

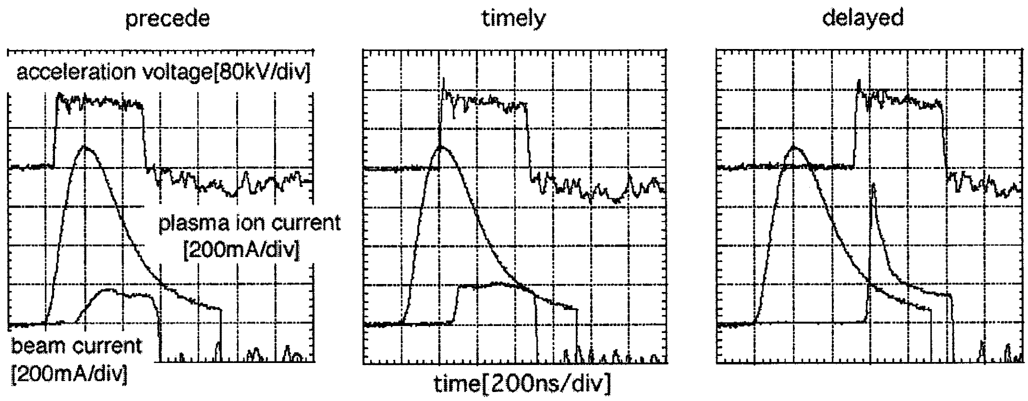

Fig. 7. Profiles of copper ion beams extracted at different timing of high-voltage supply. Time profiles of induction voltage and plasma ion current are depicted for comparison.

bremsstrahlung for the plasma formation in the present work. The emittance value of 0.05 πmm-mrad obtained in the low-voltage extraction after the 65 cm drift gives a measure of the maximum ion temperature of 4 eV (Brown, 1989), which does not contradict the electron temperature of ~2 eV measured with the single probe method as shown in Figure 3. This is because the emittance is increased by several conditions such as the space charge effect, the aberration in the extraction field, the nonideal beam optics, and so on. On the other hand, the normalized emittance observed in the high-voltage extraction using the frequency-doubled Nd:YAG laser exhibited the lowest value of 0.8 πmm-mrad at a laser energy of 53 mJ as displayed in Figure 8. This significant discrepancy between two different conditions of the ion extraction originates partially from the difference of the laser wavelength, that is, the Nd:YAG laser of $\lambda = 532$ nm produces the plasma with a temperature higher by a factor of three than the KrF of $\lambda = 248$ nm laser does via the equation $T_e \propto \lambda^{4/3}$. The factor of three in temperature contributes to the emittance increase only by $\sqrt{3}$ due to $\varepsilon \propto \sqrt{kT_i}$, where ε, k, and T_i are normalized root-mean-square emittance, Boltzmann constant, and plasma ion temperature, respectively. Here we assume that the electron temperature is proportional to the ion temperature. It is noted that the ion source with the low-voltage extraction had the long drift space for the expanding plasma. In this case, we collected the ions that had the lower transverse velocities after the expansion of 65 cm. This procedure corresponded to selection of the cold ions. On the contrary, the ion source mounted on the induction adder had no drift space. So a large fraction of the ions in the ablation plasma were extracted without selection of the transverse velocities. The configuration of the ion source without the drift space yielded the higher emittance as long as the aperture size of the cathode was the same as that of the ion source with sufficient drift space.

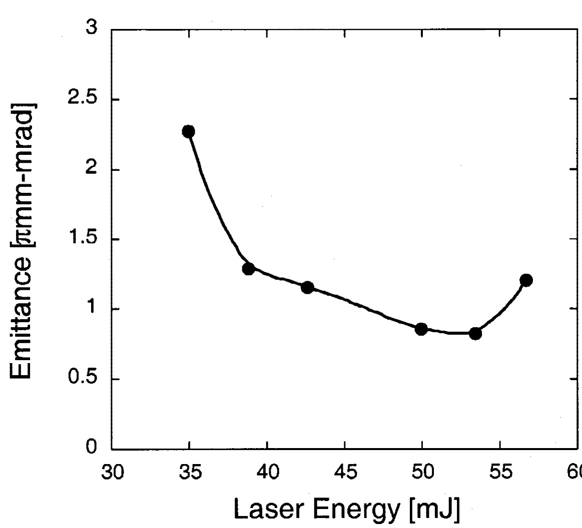

Fig. 8. Normalized emittance of copper ion beams measured as a function of irradiation energy of Nd:YAG laser. Copper ions were extracted with 150 kV pulse voltage.

In this study, we extracted $\sim 2 \times 10^{12}$ and 5×10^{12} copper ions at the extraction voltages of ~20 kV and 150 kV, respectively. These numbers of the ions are smaller by one order of magnitude than the ion number of 10^{14} per pulse required for the HIF application.

4. SUMMARY

We have examined a laser ion source at two extraction modes, that is, low-voltage DC extraction and high-voltage pulse extraction. We have extracted the low-charged copper ions consisting predominantly of Cu^{+} and Cu^{2+} with the intensity near the space charge limited current. The electron temperature T_e of the ablation plasma formed with the KrF excimer laser was measured to be ~2 eV depending on the laser power density as $T_e \propto I^{2/3}$, which verified the inverse bremsstrahlung in the plasma formation. The electron temperature observed with the single probe was consistent with the temperature derived from the measured emittance of ~0.05 πmm-mrad. This low emittance of the laser ion source operated with the low-power UV laser meets the requirement for the HIF ion

https://doi.org/10.1017/S0263034603214233 Published online by Cambridge University Press

source. However, its beam intensity is insufficient by one order of magnitude for the HIF requirement.

The larger emittance was observed for the ion source mounted on the high-voltage induction adder compared with the ion source of the low-voltage mode. This difference in the emittance was understood in terms of selection of the transverse velocities because the source of the low-voltage mode had the drift space of 65 cm and the source of the high-voltage mode had no drift space. We conclude that the drift space played an important role in selecting the low transverse velocities of the ions, that is, in selecting the cold ions.

ACKNOWLEDGMENT

This work was supported in part by Grant-in Aid for Scientific Research of the Japanese Ministry of Education No. 11480122.

NOTE ADDED IN PROOF

The ion currents shown in Figures 2 and 6 were measured without suppression of the secondary electrons because we found no obvious difference with the suppression of up to −200 V. However, we observed the decrease of the peak current by 10% at the suppression voltage of −2 kV in the measurement performed after the submission of the manuscript.

REFERENCES

Amoruso, S., Armenate, M., Berardi, V., Bruzzese, R., Pica, G. & Velotta, R. (1996). Charged species analysis as a diagnostic tool for laser produced plasma characterization. *Appl. Surf. Sci.* **106**, 507–512.

Bangerter, R.O. (1999). Status of the US heavy ion fusion program. *Fusion Eng. Des.* **44**, 71–79.

Brown, I.G. (1989). *The Physics and Technology of Ion Sources*. New York: John Wiley & Sons.

Hasegawa, J., Yoshida, M., Oguri, Y., Ogawa, M., Nakajima, M. & Horioka, K. (2000). High-current laser ion source for induction accelerators. *Nucl. Instrum. Methods B* **161–163**, 1104–1107.

Henkelmann, T., Korschinek, G., Belayev, G., Dubenkov, V., Golubev, A., Latyshev, S., Sharkov, B., Shmshurov, A. & Wolf, B. (1992). Charge state distribution of tantalum ions produced simultaneously by CO_2 and Nd:YAG laser from a laser ion source. *Rev. Sci. Instrum.* **63**, 2828–2830.

Mora, P. (1982). Theoretical model of absorption of laser light by a plasma. *Phys. Fluids* **25**, 1051–1056.

Roudskoy, I. *et al.* (1996). General feature of highly charged ion generation in laser produced plasmas. *Laser Part. Beams* **14**, 369–384.

Sharkov, B.Y., Kondrashev, S., Roudskoy, I., Savin, S., Shumshurov, A., Haseroth, H., Kugler, H., Langbein, K., Lisi, N., Magnusson, H., Scrivens, R., Schnuringer, J.C., Tambini, J., Homenko, S., Makarov, K., Roerich, V., Stepanov, A. & Satov, Y. (1998). Laser ion source for heavy ion synchrotrons. *Rev. Sci. Instrum.* **69**, 1035–1039.

Tyrrell, G.C., Coccia, L.G., York, T.H. & Boyd, I.W. (1996). Energy-dispersive mass spectrometry of high energy ions generated during KrF excimer and frequency-doubled Nd:YAG laser ablation of metals. *Appl. Surf. Sci.* **96–98**, 227–232.

Von Gutfeld, R.J. & Drefus, R.W. (1989). Electric probe measurements of pulsed ablation at 248 nm. *Appl. Phys. Lett.* **54**, 1212–1214.

Wang, J.G., Wang, D.X. & Reser, M. (1991). Beam emittance measured by the pepper-pot method. *Nucl. Instrum. Methods A* **307**, 190–194.

Weaver, I., Martin, G.W., Graham, W.G., Morrow, T. & Lewis, C.L.S. (1999). The Langmuir probe as a diagnostic of the electron component within low temperature laser ablated plasma plumes. *Rev. Sci. Instrum.* **70**, 1801–1805.

Yoshida, M., Hasegawa, J., Fukata, S., Oguri, Y., Ogawa, M., Nakajima, M., Horioka, K. & Shiho, M. (2000). Development of a high-current laser ion source for induction accelerators. *Rev. Sci. Instrum.* **71**, 1216–1218.

Yoshida, M., Hasegawa, J., Fukata, S., Oguri, Y., Ogawa, M., Nakajima, M., Horioka, K., Maebara, S. & Shiho, M. (2001). A simple time-resolved emittance measurement of a laser ion source with a digital camera. *Nucl. Instrum. Methods A* **464**, 582–586.